

## THE ABUNDANCE OF BULLET-GROUPS IN $\Lambda$ CDM

J. G. FERNÁNDEZ-TRINCADO<sup>1,2,3</sup>, J. E. FORERO-ROMERO<sup>1</sup>, T. VERDUGO<sup>3</sup>, G. FOEX<sup>4</sup> AND V. MOTTA<sup>4</sup>

<sup>1</sup> Departamento de Física, Universidad de los Andes, Cra. 1 No. 18A-10, Edificio Ip, Bogotá, Colombia

<sup>2</sup> Institute Utinam, CNRS UMR6213, Université de Franche-Comté, OSU THETA de Franche-Comté-Bourgogne, Besançon, France

<sup>3</sup> Centro de Investigaciones de Astronomía, AP 264, Mérida 5101-A, Venezuela

<sup>4</sup> Instituto de Física y Astronomía, Universidad de Valparaíso, Avda. Gran Bretaña 1111, Playa Ancha, Valparaíso 2360102, Chile

Submitted for publication in *ApJL*

### ABSTRACT

We estimate the expected distribution of displacements between the two dominant dark matter density peaks and between baryons and dark matter in halos simulated within a full cosmological context. We use as a benchmark the observation of SL2S J08544-0121, which is the lowest mass system observed so far featuring a bi-modal dark matter distribution with a dislocated baryonic component. We extend previous results by studying two halo samples: groups and clusters. We find that  $(55 \pm 5)\%$  of the dark matter halos with circular velocities in the range  $300 \text{ km s}^{-1}$  to  $700 \text{ km s}^{-1}$  (groups) show multimodal morphologies with displacements between the dark matter clumps equal or larger than  $133 \pm 21 h^{-1} \text{ kpc}$  as observed in SL2S J08544-0121. For dark matter halos with circular velocities larger than  $700 \text{ km s}^{-1}$  (clusters) this fraction rises to  $(82 \pm 3)\%$ . Using the same simulation we estimate the dark matter-to-baryon spatial separation and find that 0.1 to 1.0% of the groups should present separations equal or larger than  $87 \pm 14 h^{-1} \text{ kpc}$  corresponding to our observational benchmark; for clusters this fraction rises to  $(7 \pm 3)\%$ , consistent with previous studies of dark matter to baryon separations. The extension of the theoretical predictions and observational results towards low mass bi-modal dark matter configurations opens up the possibility for a new statistical test of  $\Lambda$ CDM.

NOTA: tomar  $186 \pm 30$  para el DM-DM displacement.

*Subject headings:* cosmology: theory – dark matter

### 1. INTRODUCTION

The Bullet Cluster (1E0657—56) provided a new kind of observational evidence for the existence of dark matter (Markevitch et al. 2004; Clowe et al. 2006). Quantifying the displacement between dark matter and the dominant baryonic component (hot X-ray emitting gas) has been used to test the Cold Dark Matter (CDM) paradigm itself by quantifying the substructure velocity required to produce such displacement (Hayashi & White 2006; Springel & Farrar 2007; Thompson & Nagamine 2012), the displacement between the dominant dark matter and baryonic component (Forero-Romero et al. 2010) to estimate the expected abundance of such events in a  $\Lambda$ CDM Universe, putting constraints on the dark matter particle self-interaction cross section and even explore possible extensions to the concordance cosmological model (Farrar & Rosen 2007; Lee & Komatsu 2010; Lee & Baldi 2012).

Since then, other examples of Bullet-like systems have been found; MACS J0025.4-1222 (Bradač et al. 2008), Abell 2744 (Merten et al. 2011), DLSCL J0916.2+2951 (Dawson et al. 2012), ZwCl 1234.0+02916 (Dahle et al. 2013). Recently (Gastaldello et al. 2014) observed a baryonic-DM displacement of  $124 \pm 20 \text{ kpc}$  in SL2S J08544-0121, a group-like system with a total mass  $2.4 \pm 0.6 \times 10^{14} M_{\odot}$ . Systems of this mass are  $\sim 10$  times more abundant than cluster systems in the mass range of the Bullet Cluster  $> 10^{15} h^{-1} M_{\odot}$ , this opens up the possibility of observationally finding bullet groups in a fair amount to impose constraints on  $\Lambda$ CDM.

However, a greater abundance of small mass systems

has to be weighted by the probability of having a merger and presenting a large displacement between the DM and baryonic components. These two conditions (merger rates, maximum possible displacement) are a function of DM halo mass in  $\Lambda$ CDM cosmologies. Such study has been performed for clusters but not for lower mass systems (Forero-Romero et al. 2010). The existence of objects like SL2S J08544-0121 and observational campaigns like the Strong Lensing Legacy Survey (SL2S) (Cabanac et al. 2007; More et al. 2012) open up the possibility of finding multi-modal dark matter distributions in the group mass range.

In this Letter we compute the abundance of group-like dark matter halos with a multi-modal morphology that also might present a DM-baryon displacement. To this end we use a N-body cosmological simulation with such a resolution that allows us to identify multi-modal dark matter distributions in hosts with circular velocities larger than  $300 \text{ km s}^{-1}$ .

This Letter is organized as follows. In Section 2 we present the simulation and the halo catalogs used in this work. We continue in Section 3 with the geometry of the problem at hand and the measurements setup. Next in Section 4 we present our results and observational perspectives to finally conclude in Section 5.

### 2. SIMULATION, HALO CATALOGS AND PAIRS

We use the Bolshoi Run, a cosmological DM only simulation over a cubic volume of  $250 h^{-1} \text{ Mpc}$  comoving on a side. The simulation uses the ART code (Kravtsov et al. 1997) to follow the evolution of a dark matter density field sampled with  $2048^3$  from  $z = 80$  to  $z = 0$ . The

cosmology used corresponds to the spatially flat concordance model with the following parameters: the density parameter for matter (dark matter and baryons)  $\Omega_m = 0.27$ , the density parameter for baryonic matter  $\Omega_b = 0.0469$ , the density parameter for dark energy  $\Omega_\Lambda = 0.73$ , the Hubble parameter  $h = 0.7$ , the normalization of the Power spectrum  $n = 0.95$  and the amplitude of mass density fluctuation (at redshift  $z=0$ )  $\sigma_8 = 0.82$ . These cosmological parameters are consistent with the nine-year Wilkinson Microwave Anisotropy Probe (WMAP) results (Hinshaw et al. 2013). A detailed presentation of the simulation can be found in Klypin et al. (2011).

The number of particles used for each of the DM component was  $2048^3$ , resulting in a mass resolution of  $1.35 \times 10^8 M_\odot h^{-1}$ . The completeness limit in this simulation is set for halos with 100 particles corresponding to a mass of  $1.35 \times 10^{10} h^{-1} M_\odot$  or a maximum circular velocity  $V_c$  of  $50 \text{ km s}^{-1}$ .

We use halo catalogs constructed using the Bound Density Maxima (BDM) algorithm (Klypin & Holtzman 1997; Klypin et al. 1999). To define the radius of a halo we use a density threshold of 360 times the mean density of the Universe (or 200 times the critical density), for different redshifts we use the overdensity criterion by Bryan & Norman (1998). An important feature of BDM is that it allows us to detect sub-halos inside larger virialized structures.

All the raw data used in this Letter is available through the Multidark database<sup>1</sup> (Riebe et al. 2013). Furthermore, in order to facilitate the reproducibility and reuse of our results we have made available all the data and the source code available in a public repository<sup>2</sup>.

In this Letter we make a study at four different redshifts  $z = 0.0, 0.25, 0.5$  and  $1.0$ . First, we select all the host halos (i.e. halos that are not inside a larger halo) with circular velocities  $V_c \geq 300 \text{ km s}^{-1} (\geq 1 \times 10^{13} h M_{\text{sun}})$ . Then, we select the sub-halos with circular velocities  $V_c \geq 75 \text{ km s}^{-1} (\geq 5 \times 10^{10} h^{-1} M_\odot)$ . The objective is to use this sub-halos as the tracer of the sub-dominant dark matter clump in the merging cluster, i.e. the bullets.

For the redshifts  $z = 0.0, 0.25, 0.5$  and  $1.0$  we find 10041, 10346, 10554 and 10382 host halos and 157853, 177331, 195072, 225188 sub-halos, respectively. These two sets (host halos and sub-halos) constitute the basis for our analysis. We associate each host halo to its most massive sub-halo, each one of these pairs (host & sub-halo) is considered as a potential Bullet system and is kept for the analysis described in the next Section.

### 3. BULLET GEOMETRY AND MEASUREMENT SETUP

The Bullet-like configurations are composed by two dark matter structures: the host halo and the dominant sub-halo. We describe the kinematics of this configuration by the position and velocity vectors of the sub-halo in a frame of reference where the main halo is at rest; thus  $\vec{v} = \vec{v}_{\text{sub}} - \vec{v}_{\text{halo}}$  and  $\vec{r} = \vec{r}_{\text{sub}} - \vec{r}_{\text{halo}}$ , where the subscripts *host* and *sub* refer to the position of the minimum of potential for the host and sub-halo in the frame of reference of the simulation, respectively.

The angle between these two vectors can be characterized by,

$$\mu \equiv \cos(\theta) = \frac{\vec{v} \cdot \vec{r}}{\|\vec{v}\| \|\vec{r}\|}. \quad (1)$$

This encodes relevant information to describe the collision, i.e. cases of  $|\mu| \approx 1$  can be considered as head-on collisions while  $|\mu| \approx 0$  describes a grazing trajectory.

The geometrical configuration can be further described by the following quantities. The circular velocity of each component,  $V_{c,\text{host}}$  for the host and  $V_{c,\text{sub}}$  for the sub-halo and the size of the host halo  $R_{\text{vir}}$ . Another useful quantity computed in the simulation is the distance between the minimum of potential for the host halo and its center of mass,  $X_{\text{off}} = \|\vec{r}_{\text{min}} - \vec{r}_{\text{cm}}\|/R_{\text{vir}}$  which serves as a measurement of how much the host halo is perturbed.

As a zero-th order approximation, in this paper we work with three observed quantities for Bullet-like systems. The projected distance between two dominant DM clumps, the projected distance between the DM-baryonic clumps and the ratio of the mass associated to the DM clumps.

From the simulation point of view, the first quantity can be translated into the 2D projected values of  $\|\vec{r}\|$  and its value relative to the virial radius  $D_{\text{off}} = \|\vec{r}\|_{2D}/R_{\text{vir}}$ . The last quantity, the mass ratio, can be approximated by ratio of the circular velocities of the two clumps  $V_{c,\text{sub}}/V_{c,\text{host}}$  which should be equal to the square root of the mass ratio. The second quantity, the projected DM-baryon distance, is not directly available from a DM-only simulation but, as we show in the Results section, can be inferred from the available information.

The physical quantities described above can be used to describe the three main stages in a bullet-like encounter. First, the sub-halo crosses the virial radius of the host halo starting a head on collision,  $\|\vec{r}\|/R_{\text{vir}} \approx 1$  and  $\mu \lesssim 0.0$ . Second, as the sub-halo crosses for the first time the center of the host halo  $\|\vec{r}\|/R_{\text{vir}} < 1.0$  and  $\mu > 0.0$ . Third, as the sub-halo reaches apogee and comes back to the center of the halo  $\|\vec{r}\|/R_{\text{vir}} < 1.0$  and  $\mu < 0.0$ . We use these quantities in the next section to fully characterize the different kind of interactions observed in the Bolshoi Run,

## 4. RESULTS

### 4.1. Displacements and Relative Circular Velocities

The main result of this paper is summarized in Figure 1, it presents the integrated probability distribution for the displacement between the center of the host halo and its dominant sub-halo. The left panel shows the displacement in physical units and the right panel as a fraction of the virial radius of the host halo.

Figure 1 shows the results for two different populations; groups with  $300 \text{ km s}^{-1} < V_{c,\text{host}} < 700 \text{ km s}^{-1}$  and clusters with  $V_{c,\text{host}} > 700 \text{ km s}^{-1}$ . Additionally, this is presented for all redshifts  $z = 0.0, 0.25, 0.5$  and  $1.0$ .

The panel with the projected 2D physical displacements also shows a vertical stripe with the estimated displacement for the Bullet-group reported by Gastaldello et al. (2014). In the group sample we see that a fraction of 50% to 60% should present a displacement equal than the estimate for SL2S J08544-0121; in the cluster

<sup>1</sup> [www.multidark.org](http://www.multidark.org)

<sup>2</sup> [https://github.com/Fernandez-Trincado/Bullet\\_Groups-2014](https://github.com/Fernandez-Trincado/Bullet_Groups-2014)

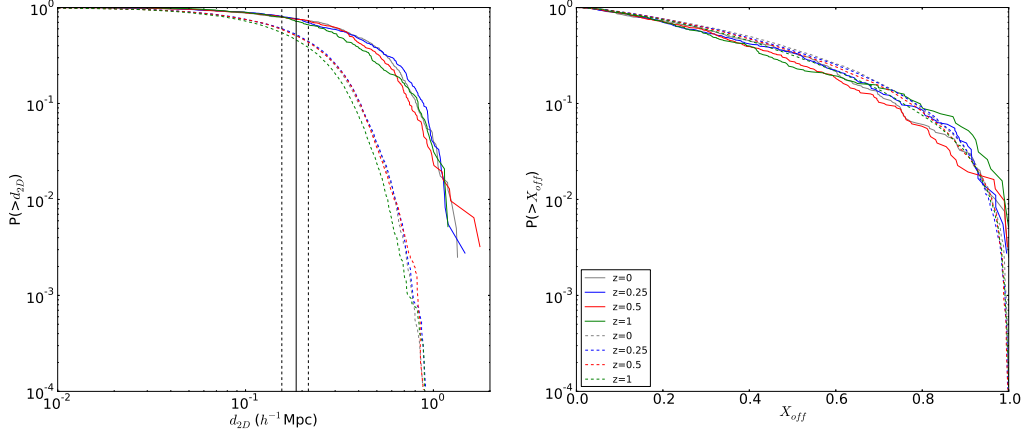


FIG. 1.— Integrated probability distribution for the displacement between the center of the host halo and its dominant sub-halo. The left panel shows the results in terms of the physical displacements while the right panel shows the displacements normalized by the virial radius of the host halo. The continuous (dashed) line corresponds to the halos in the cluster (group). The vertical lines show the mean value and uncertainties ( $133 \pm 21 h^{-1} \text{ kpc}$ ) in the separation between the two dark matter clumps estimated in Gastaldello et al. (2014) for the SL2S J08544-0121. Between 50% to 60% of the groups show a displacement equal or larger than this observational benchmark.

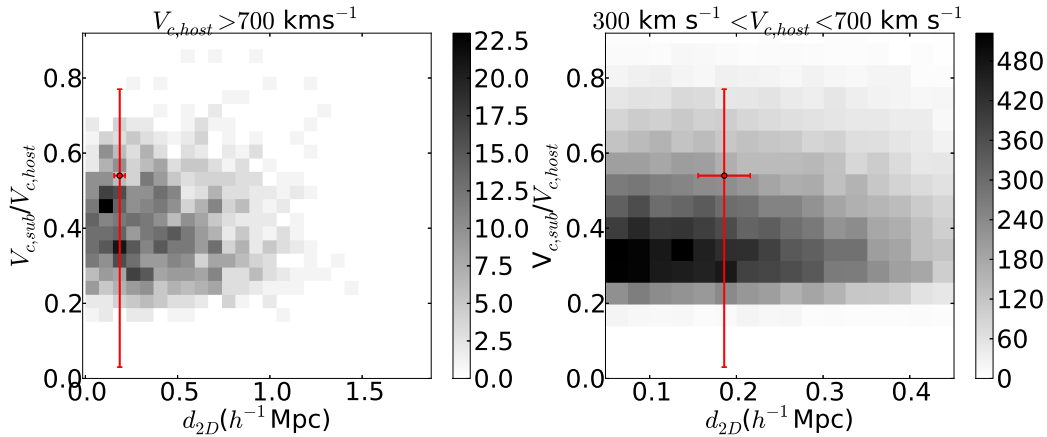


FIG. 2.— 2D histogram in the plane  $V_{c,\text{sub}}/V_{c,\text{host}}-d_{2D}$ . The left panel corresponds to clusters and the right panel to groups. The star with error bars corresponds to SL2S J08544-0121 data reported from Muñoz et al. (2013) and Gastaldello et al. (2014). The data used to construct the histograms integrates the objects at all redshifts.

sample this fraction increases to 80%-85%. The uncertainties in this estimates are derived from the uncertainties in the displacement measurement for SL2S J08544-0121. This fraction is naturally higher in more massive systems because they are larger in size. Normalizing the displacements by the virial radius, right panel Figure 1, we see that the distribution is the same regardless of the sample and the redshift.

Figure 2 shows 2D histograms in a plane defined by the ratio of the two circular velocities  $V_{c,\text{sub}}/V_{c,\text{host}}$  and the projected 2D physical displacements; quantities that can be constrained by observations.

To construct this figure we co-add all the halos in the sample (left, clusters; right, groups) at all redshifts. We stack the data because we do not observe any strong redshift dependence. This allows us to increase the signal in each bin. We overplot a star with error bars that represents the observational constraints for the system SL2S J08544-0121 using the fraction in velocity disper-

sion in the line-of-sight of the group SL2S SJ08544-0121 ( $\sigma_{\text{host}} = 341^{+43}_{-109} \text{ km s}^{-1}$  and  $\sigma_{\text{sub}} = 185^{+30}_{-62} \text{ km s}^{-1}$ ) reported by Muñoz et al. (2013) and the DM displacement inferred from the data presented by Gastaldello et al. (2014).

#### 4.2. Collision Geometries

Figure 3 presents the geometry of the bullet groups using the variables  $\mu$  and  $D_{\text{off}}$ . The first evident feature is that most of the configurations have  $|\mu| > 0.9$  ( $\theta \leq 30^\circ$ ), meaning that most of the collisions can be described as a head-on encounter while only a minority with  $|\mu| < 0.9$  have grazing trajectories. For the pairs on radial trajectories there are three regions of interest in this plane that describe different stages in the collision, assuming that the sub-halo merges (or falls below the BDM detection threshold) right at its second pass through the center of the host halo (Poole et al. 2006).

The first region has  $\mu \approx -1$  and  $D_{\text{off}} > 0.6$ , which

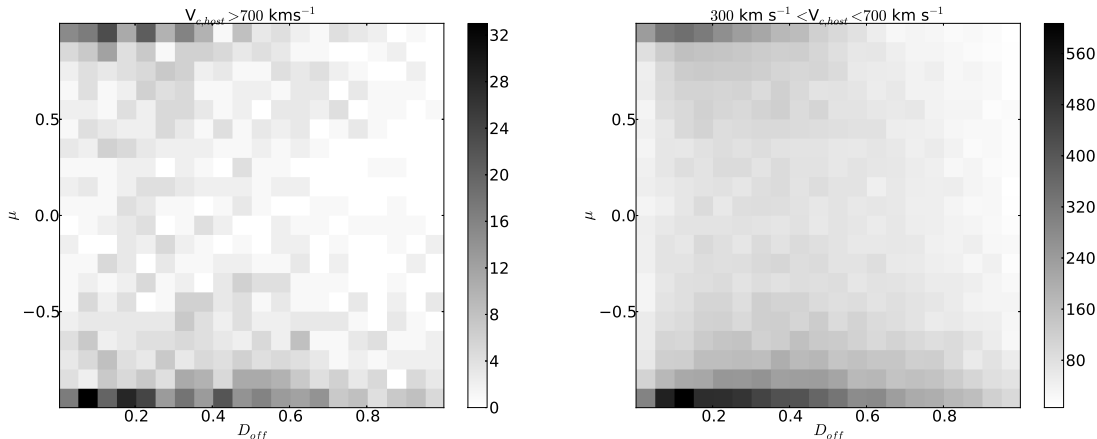


FIG. 3.— 2D histograms in the plane  $\mu$ - $D_{\text{off}}$ . The left panel corresponds to clusters and the right panel to groups. The data used to construct this histogram includes the halos at all redshifts.

locates the systems where a head-on collision has just started. The sub-halo is close to the boundary of the host halo and is infalling. The second region has  $\mu \approx 1$  and  $D_{\text{off}} < 0.6$ ; at this stage the collision continues after the first crossing of the host's center, the low number of halos with radial infalling velocities and displacements  $D_{\text{off}} > 0.6$  suggest that this is the maximum range of radii for the apogee. The third region corresponds to  $\mu \approx -1$  and  $D_{\text{off}} < 0.6$  that is the secondary infall after apogee. We use this sequence in the next subsection to estimate the expected displacement between baryons and the dominant DM clump.

#### 4.3. Displacement between Dark Matter and Baryons

Strictly speaking, the results we have derived so far apply to multi-modal groups and their expected separation between the two dominant dark matter clumps. However, a non-zero DM-DM displacement cannot be interpreted as having a corresponding non-zero DM-baryon displacement. Given that we use a DM only simulation, we have to find a way to estimate DM-baryon displacements from the available information.

This estimate is based on the different collision stages described at the end of the previous sub-section. For instance, in systems where the halo is starting to fall into the host ( $\mu \approx -1$ ,  $D_{\text{off}} > 0.6$ ) the DM-baryon displacement should be equal to zero. However, when the sub-structure has already passed through the center of the host halo, i.e. cases where  $\mu \approx 1$ , the DM-baryon displacement should be different from zero.

To estimate the DM-baryon displacement we work under the following hypothesis. First, we consider that systems with  $|\mu| < 0.9$  have a baryonic displacement,  $d_{2D}^{\text{bar}}$ , equal to zero. This means that only head-on encounters produce a displacement. Second, we consider that all systems with infalling velocities  $\mu < -0.9$  and large displacements  $D_{\text{off}} > 0.6$  also have baryonic displacements equal to zero. Third, for all the other cases we estimate the displacement between the baryons and the dominant DM peak by  $d_{2D}^{\text{bar}} = X_{\text{off}} R_{\text{vir}}$ , where  $X_{\text{off}}$  is the offset

computed between the minimum of potential and the center of mass for each host halo computed from all the matter inside the virial radius.

This simplified model does not take into account that there is a fraction of halos with  $\mu < -0.9$  and  $D_{\text{off}} < 0.6$  for which the collision has not started and should have  $d_{2D}^{\text{bar}} = 0$ . A detailed modeling of this fraction requires the study of the complete merger tree of the halo and sub-halo, a study beyond the scope of this Letter. Instead we caution the reader that the derived fraction of halos with a displacement  $< d_{2D}^{\text{bar}}$  can be considered as an upper limit.

The results for the integrated distributions for  $> d_{2D}^{\text{bar}}$  are shown in Figure 4. The dashed lines represented the results for groups and the continuous lines correspond to clusters. As a test of our model we compare the cluster results against the analytic fit provided by Forero-Romero et al. (2010). This fit reproduces the statistics for the DM-baryon separation found for clusters more massive than  $> 10^{14} h^{-1} M_{\odot}$  in a simulation which included a description for DM and gas with 8 times the volume of the Bolshoi Simulation. The fit is valid for separations larger than  $70 h^{-1} \text{kpc}$ , beyond which we find that it provides a remarkably good description within a factor of  $\sim 2$  of our results. This gives us confidence in our approach to estimate the expected fraction of groups with a DM-baryon displacement.

From Figure 4 we see that only a fraction of 0.1% to 1% of the groups are expected to have a DM-baryon displacement equal or larger than  $87 \pm 14 h^{-1} \text{kpc}$  as observed in SL2S J08544-0121. This fraction rises to 4% to 10% in the case of clusters, consistent with the results reported by Forero-Romero et al. (2010).

#### 4.4. Possible Observational Statistical Tests

Recently (Foëx et al. 2013) presented an analysis of 80 galaxy groups from the SL2S sample. From the light distribution, only 34 objects ( $\sim 42\%$ ) have regular isophotes, 33 had elongated isophotes (hints of merging system), and 13 ( $\sim 16\%$ ) had a clear bi-modal light



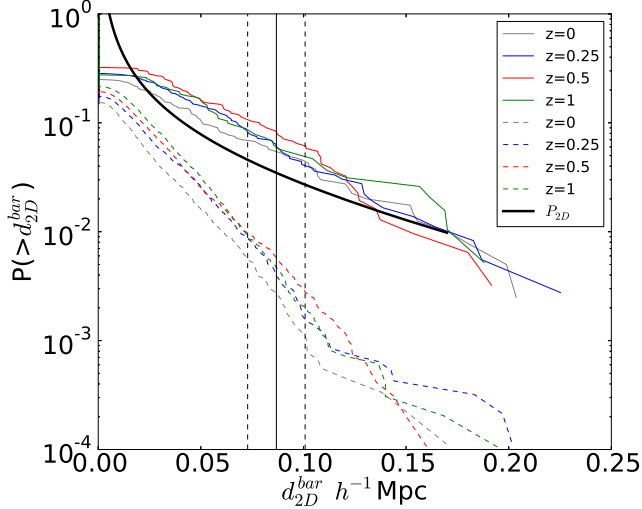


FIG. 4.— Integrated probability distribution for the estimated baryonic displacements in the group and cluster samples. Continuous (dashed) lines correspond to clusters (groups). The continuous black line marked as  $P_{2D}$  shows the statistics reported by Forero-Romero et al. (2010) for a cosmological simulation including DM and baryons. The vertical lines correspond to the mean value and uncertainty of the displacement measured for SL2S J08544-0121.

distribution.

The bi-modal objects are defined to have at least a clear second luminosity peak within  $350h^{-1}\text{kpc}$  from the main halo, as traced by the strong lensing system. The lowest separation in those systems is  $64h^{-1}\text{kpc}$  and the average is  $145 \pm 52h^{-1}\text{kpc}$ . Comparing this average displacement against the integrated distribution for the group sample (left panel, Figure 1) one would expect between 40% to 80% of DM halos to present those displacements. This fraction is certainly larger than the  $\approx 16\%$  inferred from the observational sample.

We have taken the results from the simulation and selected all the objects in the group sample with a DM-DM displacement less than  $350h^{-1}\text{kpc}$  but larger than  $64h^{-1}\text{kpc}$  to find XXX objects in total. From this subsample we find that XXX have a DM-baryon displacement larger than  $87h^{-1}\text{kpc}$ .

This rough comparison hints that it is possible to find a large fraction of multi-modal groups with a DM-baryon displacement in a  $\Lambda\text{CDM}$  cosmology. A proper comparison must take into account all the observational uncertainties and biases to derive a stronger prediction from the simulation, something that is beyond the scope of this Letter.

## 5. CONCLUSIONS

In this Letter we estimate fraction of galaxy groups and clusters that can present observational features associated to a bullet-like event. This is motivated by the recent observational results of (Gastaldello et al. 2014) where a system (SL2S J08544-0121) on the mass range  $1 \times 10^{14}h^{-1}M_{\odot}$  and velocity dispersion  $650\text{ km s}^{-1}$  was reported to feature a displacement between its baryonic (hot gas) and dark matter components.

We estimate the distribution of projected displacements between the dominant DM clumps in two kinds of systems; groups with circular velocities  $300\text{ km s}^{-1} < V_c < 700\text{ km s}^{-1}$  ( $1.0 \times 10^{13}h^{-1}M_{\odot} < M_{\text{vir}} < 1.0 \times 10^{14}h^{-1}M_{\odot}$ ) and clusters with  $V_c > 700\text{ km s}^{-1}$  ( $M_{\text{vir}} > 1.0 \times 10^{14}h^{-1}M_{\odot}$ ). We report these results at four different redshifts  $z = 0.0, 0.25, 0.5$  and  $1.0$ . Our results are based on large DM-only N-body cosmological simulation with a resolution that allows to study for the first time Bullet-like configurations in the mass range of galaxy groups.

Our main results is that that a fraction of 50%-60% of the halos in the group sample present displacement equal or larger than the observed displacement for SL2S J08544-0121. For halos in the cluster sample this fraction increases to 80%-85%. We also derive an estimate for the displacement between the DM and the baryonic component. In the group sample 0.1%-1.0% of the halos show a displacement equal or larger than the measurements of SL2S J08544-0121 by (Gastaldello et al. 2014). In the cluster sample this fraction rises to 4%-10%.

We also find distributions for the DM separation and the velocity of the bullet through its host. If these quantities are normalized by the virial radius and the circular velocity, respectively, we arrive at distributions close to universal that are similar for the two halo samples at all redshifts.

For the case of SL2S J08544-0121 a fair comparison is achieved against cluster sample, which has statistics dominated by objects of similar mass. In this case we conclude that the existence of such configuration is highly probable in  $\Lambda\text{CDM}$  (4% to 10% abundance). In turn, for the same separation the fraction for groups is lower (0.1% to 1%). Taking into account that the difference in spatial abundance between these two samples is on the order of a factor of 10, one can conclude that the absolute number of groups and clusters presenting a DM-baryon displacement larger or equal to SL2S J08544-0121 should be of the same order.

An observational possibility opens up with surveys such as SL2S that targetted a large number of groups and estimate its multi-modal nature from lensing analysis (Foëx et al. 2013), an approach that can be exploited with upcoming lensing surveys (e.g. with the *Euclid* satellite).

The CosmoSim database used in this paper is a service by the Leibniz-Institute for Astrophysics Potsdam (AIP). The Bolshoi simulation was performed within the Bolshoi project of the University of California High-Performance AstroComputing Center (UC-HIPACC) and was run at the NASA Ames Research Center.

J.E.F-R acknowledges support from Vicerrectoría de Investigaciones through a FAPA starting grant.

T.V. acknowledges support from CONACYT through grant 165365 and 203489 through the program Estancias posdoctorales y sabáticas al extranjero para la consolidación de grupos de investigación.

V.M. gratefully acknowledges FONDECYT support through grant 1120741 and ECOS/CONICYT through

## REFERENCES

Bradač, M., Allen, S. W., Treu, T., Ebeling, H., Massey, R., Morris, R. G., von der Linden, A., & Applegate, D. 2008, *ApJ*, 687, 959

Bryan, G. L., & Norman, M. L. 1998, *ApJ*, 495, 80

- Cabanac, R. A., Alard, C., Dantel-Fort, M., Fort, B., Gavazzi, R., Gomez, P., Kneib, J. P., Le Fèvre, O., Mellier, Y., Pello, R., Soucail, G., Sygnet, J. F., & Valls-Gabaud, D. 2007, *A&A*, 461, 813
- Clowe, D., Bradač, M., Gonzalez, A. H., Markevitch, M., Randall, S. W., Jones, C., & Zaritsky, D. 2006, *ApJ*, 648, L109
- Dahle, H., Sarazin, C. L., Lopez, L. A., Kouveliotou, C., Patel, S. K., Rol, E., van der Horst, A. J., Fynbo, J., Wijers, R. A. M. J., Burrows, D. N., Gehrels, N., Grupe, D., Ramirez-Ruiz, E., & Michałowski, M. J. 2013, *ApJ*, 772, 23
- Dawson, W. A., Wittman, D., Jee, M. J., Gee, P., Hughes, J. P., Tyson, J. A., Schmidt, S., Thorman, P., Bradač, M., Miyazaki, S., Lemaux, B., Utsumi, Y., & Margoniner, V. E. 2012, *ApJ*, 747, L42
- Farrar, G. R., & Rosen, R. A. 2007, *Physical Review Letters*, 98, 171302
- Foëx, G., Motta, V., Limousin, M., Verdugo, T., More, A., Cabanac, R., Gavazzi, R., & Muñoz, R. P. 2013, *A&A*, 559, A105
- Forero-Romero, J. E., Gottlöber, S., & Yepes, G. 2010, *ApJ*, 725, 598
- Gastaldello, F., Limousin, M., & Foëx, G. 2014, *MNRAS* submitted
- Hayashi, E., & White, S. D. M. 2006, *MNRAS*, 370, L38
- Hinshaw, G., Larson, D., Komatsu, E., Spergel, D. N., Bennett, C. L., Dunkley, J., Nolte, M. R., Halpern, M., Hill, R. S., Odegard, N., Page, L., Smith, K. M., Weiland, J. L., Gold, B., Jarosik, N., Kogut, A., Limon, M., Meyer, S. S., Tucker, G. S., Wollack, E., & Wright, E. L. 2013, *ApJS*, 208, 19
- Klypin, A., Gottlöber, S., Kravtsov, A. V., & Khokhlov, A. M. 1999, *ApJ*, 516, 530
- Klypin, A., & Holtzman, J. 1997, *ArXiv Astrophysics e-prints*
- Klypin, A. A., Trujillo-Gomez, S., & Primack, J. 2011, *ApJ*, 740, 102
- Kravtsov, A. V., Klypin, A. A., & Khokhlov, A. M. 1997, *ApJS*, 111, 73
- Lee, J., & Baldi, M. 2012, *ApJ*, 747, 45
- Lee, J., & Komatsu, E. 2010, *ApJ*, 718, 60
- Markevitch, M., Gonzalez, A. H., Clowe, D., Vikhlinin, A., Forman, W., Jones, C., Murray, S., & Tucker, W. 2004, *ApJ*, 606, 819
- Merten, J., Coe, D., Dupke, R., Massey, R., Zitrin, A., Cypriano, E. S., Okabe, N., Frye, B., Braglia, F. G., Jiménez-Teja, Y., Benítez, N., Broadhurst, T., Rhodes, J., Meneghetti, M., Moustakas, L. A., Sodré, Jr., L., Krick, J., & Bregman, J. N. 2011, *MNRAS*, 417, 333
- More, A., Cabanac, R., More, S., Alard, C., Limousin, M., Kneib, J.-P., Gavazzi, R., & Motta, V. 2012, *ApJ*, 749, 38
- Muñoz, R. P., Motta, V., Verdugo, T., Garrido, F., Limousin, M., Padilla, N., Foëx, G., Cabanac, R., Gavazzi, R., Barrientos, L. F., & Richard, J. 2013, *A&A*, 552, A80
- Poole, G. B., Fardal, M. A., Babul, A., McCarthy, I. G., Quinn, T., & Wadsley, J. 2006, *MNRAS*, 373, 881
- Riebe, K., Partl, A. M., Enke, H., Forero-Romero, J., Gottlöber, S., Klypin, A., Lemson, G., Prada, F., Primack, J. R., Steinmetz, M., & Turchaninov, V. 2013, *Astronomische Nachrichten*, 334, 691
- Springel, V., & Farrar, G. R. 2007, *MNRAS*, 380, 911
- Thompson, R., & Nagamine, K. 2012, *MNRAS*, 419, 3560